

# Timelike DVCS in Ultraperipheral Collisions

Jakub Wagner

Theoretical Physics Department  
National Center for Nuclear Research

CERN, 2 June 2014

DVCS:

M. Diehl - Phys.Rept. 388 (2003),

M. Guidal, H. Moutarde, M. Vanderhaeghen - Rept.Prog.Phys. 76 (2013),

P. Kroll, H. Moutarde, F. Sabatie - Phys. Rev. D87 (2013),

timelike-DVCS:

E. R. Berger, M. Diehl, B. Pire - Eur.Phys.J. C23 (2002)

B. Pire, L. Szymanowski and JW - Phys.Rev. D79 (2009),

B. Pire, L. Szymanowski and JW - Phys. Rev. D83 (2011),

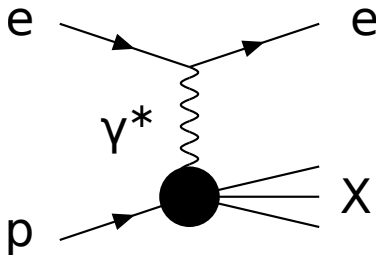
D. Mueller, B. Pire, L. Szymanowski and JW - Phys. Rev. D86 (2012),

H. Moutarde, B. Pire, F. Sabatié, L. Szymanowski and JW - Phys. Rev. D87 (2013),

A. Goritschnig, B. Pire and JW - arXiv:1404.0713 [hep-ph] - Phys. Rev. D?? (2014)



## Deep Inelastic Scattering $ep \rightarrow eX$



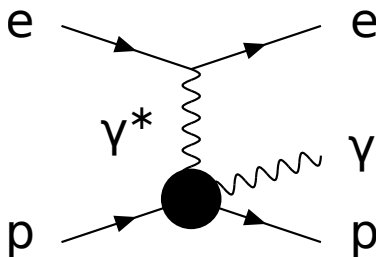
In the **Björken limit** i.e. when the photon virtuality  $Q^2 = -q^2$  and the squared hadronic c.m. energy  $(p + q)^2$  become large, with the ratio  $x_B = \frac{Q^2}{2p \cdot q}$  fixed, the cross section factorizes into a **hard partonic subprocess** calculable in the perturbation theory, and a **parton distributions**.



- ▶ Parton distributions encode the distribution of **longitudinal** momentum and polarization carried by quarks, antiquarks and gluons within fast moving hadron
- ▶ PDFs don't provide information about how partons are distributed in the **transverse** plane and ...
- ▶ about how important is the **orbital angular momentum** in making up the total spin of the nucleon.
- ▶ Recently - growing interest in the **exclusive** scattering processes, which may shed some light on these issues through the **generalized parton distributions (GPDs)** .



The simplest and best known process is **Deeply Virtual Compton Scattering**:  
 $ep \rightarrow ep\gamma$



Factorization into GPDs and perturbative coefficient function - on the level of amplitude.

DIS :  $\sigma = \text{PDF} \otimes \text{partonic cross section}$   
 DVCS :  $\mathcal{M} = \text{GPD} \otimes \text{partonic amplitude}$



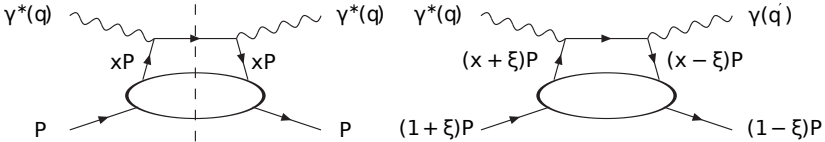


Figure: Deep Inelastic Scattering cross section is given by the **imaginary part** of diagram (a). Amplitude of Deeply Virtual Compton Scattering is given by diagram (b).



## Symmetric variables

$$P = \frac{p + p'}{2} \quad , \quad \bar{q} = \frac{q + q'}{2}$$

Generalized Bjorken variable:

$$\xi = \frac{-\bar{q}^2}{2\bar{q} \cdot P} \approx \frac{x_B}{2 - x_B} \quad , \quad x_B = \frac{Q^2}{2q \cdot p}$$

momentum transfer between proton initial and final state:

$$t = (p' - p)^2$$

In the convenient reference frame, where  $P$  has only positive time- and z-components, and light vector are defined as:

$$v_+ = (1, 0, 0, 1) \frac{1}{\sqrt{2}} \quad , \quad v_- = (1, 0, 0, -1) \frac{1}{\sqrt{2}}$$

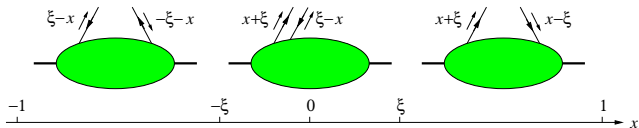
$(-2\xi)$  has an interpretation of the fraction of momentum transport in "+" direction.



## GPD definition.

$$\begin{aligned} F^q &= \frac{1}{2} \int \frac{dz^-}{2\pi} e^{ixP^+z^-} \langle p' | \bar{q}(-\frac{1}{2}z) \gamma^+ q(\frac{1}{2}z) | p \rangle \Big|_{z^+=0, \mathbf{z}=0} \\ &= \frac{1}{2P^+} \left[ H^q(x, \xi, t) \bar{u}(p') \gamma^+ u(p) + E^q(x, \xi, t) \bar{u}(p') \frac{i\sigma^{+\alpha} \Delta_\alpha}{2m} u(p) \right], \\ F^g &= \frac{1}{P^+} \int \frac{dz^-}{2\pi} e^{ixP^+z^-} \langle p' | G^{+\mu}(-\frac{1}{2}z) G_\mu^+(\frac{1}{2}z) | p \rangle \Big|_{z^+=0, \mathbf{z}=0} \\ &= \frac{1}{2P^+} \left[ H^g(x, \xi, t) \bar{u}(p') \gamma^+ u(p) + E^g(x, \xi, t) \bar{u}(p') \frac{i\sigma^{+\alpha} \Delta_\alpha}{2m} u(p) \right], \end{aligned}$$

- interpretation, ERBL, DGLAP



- Three variables  $x, \xi, t$ .

## GPD - properties,

- ▶ Forward limit:

$$\begin{aligned}H^q(x, 0, 0) &= q(x), & \text{for } x > 0, \\H^q(x, 0, 0) &= -\bar{q}(x), & \text{for } x < 0, \\H^g(x, 0, 0) &= xg(x),\end{aligned}$$

similarly for polarized distributions and PDFs.

- ▶ Reduction to form factors:

$$\int_{-1}^1 dx H^q(x, \xi, t) = F_1^q(t), \quad \int_{-1}^1 dx E^q(x, \xi, t) = F_2^q(t),$$

where the Dirac and Pauli form factors

$$\langle p' | \bar{q}(0) \gamma^\mu q(0) | p \rangle = \bar{u}(p') \left[ F_1^q(t) \gamma^\mu + F_2^q(t) \frac{i\sigma^{\mu\alpha} \Delta_\alpha}{2m} \right] u(p),$$

- ▶ Ji sum rule:

$$\lim_{t \rightarrow 0} \int_{-1}^1 dx x [H_f(x, \xi, t) + E_f(x, \xi, t)] = 2J_f$$

where  $J_f$  is fraction of the proton spin carried by quark  $f$  (including spin and orbital angular momentum).

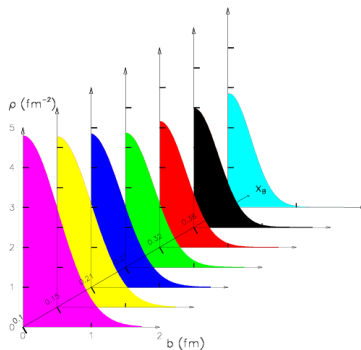


## Impact parameter representation

At  $\xi = 0 \quad \Rightarrow \quad -t = \Delta_{\perp}^2 :$

$$H(x, \mathbf{b}_{\perp}) = \int \frac{d^2 \Delta_{\perp}}{(2\pi)^2} e^{-i\mathbf{b}_{\perp} \cdot \Delta_{\perp}} H(x, 0, -\Delta_{\perp})$$

can be interpreted as probability of finding a parton with longitudinal momentum fraction  $x$  at a given  $\mathbf{b}_{\perp}$ .

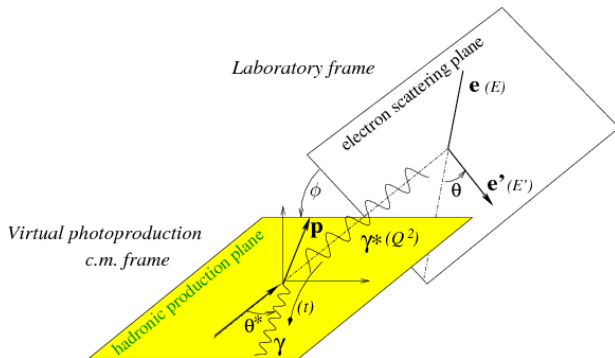


- ▶ GPDs enter factorization theorems for hard **exclusive** reactions (DVCS, deeply virtual meson production, TCS etc.), in a similar manner as PDFs enter factorization theorems for **inclusive** (DIS, etc.)
- ▶ GPDs are functions of  $x, t, \xi, \mu_F^2$
- ▶ First moment of GPDs enters the Ji's sum rule for the **angular momentum** carried by partons in the nucleon,
- ▶ 2+1 **imaging** of nucleon,
- ▶ Deeply Virtual Compton Scattering (**DVCS**) is a golden channel for GPDs extraction,



## DVCS - variables

Four variables needed to describe  $ep \rightarrow ep\gamma$  at fixed beam energy. Usually :  $Q^2, x_B, t$  and  $\phi$ :



## Coefficient functions and Compton Form Factors

CFFs are the GPD dependent quantities which enter the amplitudes. They are defined through relations:

$$\mathcal{A}^{\mu\nu}(\xi, t) = -e^2 \frac{1}{(P+P')^+} \bar{u}(P') \left[ g_T^{\mu\nu} \left( \mathcal{H}(\xi, t) \gamma^+ + \mathcal{E}(\xi, t) \frac{i\sigma^{+\rho} \Delta_\rho}{2M} \right) + i\epsilon_T^{\mu\nu} \left( \tilde{\mathcal{H}}(\xi, t) \gamma^+ \gamma_5 + \tilde{\mathcal{E}}(\xi, t) \frac{\Delta^+ \gamma_5}{2M} \right) \right] u(P),$$

,where:

$$\mathcal{H}(\xi, t) = + \int_{-1}^1 dx \left( \sum_q T^q(x, \xi) H^q(x, \xi, t) + T^g(x, \xi) H^g(x, \xi, t) \right)$$

GPDs enter through convolutions! At LO in  $\alpha_S$ :

$$DVCS T^q = -e_q^2 \frac{1}{x + \xi - i\epsilon} - (x \rightarrow -x)$$

$$DVCS \text{Re}(\mathcal{H}) \sim P \int \frac{1}{x + \xi} H^q(x, \xi, t), \quad DVCS \text{Im}(\mathcal{H}) \sim i\pi H^q(\xi, \xi, t)$$

# DVCS and BH

Figure 12 from Michel Guidal et al 2013 Rep. Prog. Phys. 76 066202

$$\sigma(ep \rightarrow ep\gamma) \propto \left[ \begin{array}{c} \text{DVCS} \\ \text{BH} \end{array} \right]^2$$

The diagram shows the cross-section  $\sigma(ep \rightarrow ep\gamma) \propto \left[ \text{DVCS} + \text{BH} \right]^2$ . The DVCS term is represented by a single diagram where an incoming electron  $e$  and proton  $p$  interact at a black vertex, producing an outgoing electron  $e'$ , proton  $p'$ , and a photon  $\gamma$ . The BH term is represented by two diagrams under a bracket, showing the exchange of a photon  $\gamma$  between the electron and proton lines. In the first BH diagram, the electron emits a photon  $\gamma$  which then interacts with the proton at the vertex. In the second BH diagram, the proton emits a photon  $\gamma$  which then interacts with the electron at the vertex. The photon lines are labeled  $\gamma^*$  where they connect to the vertex and  $\gamma$  where they are emitted or absorbed.



## Observables

The  $lp \rightarrow lp\gamma$  cross section on an unpolarized target for a given beam charge  $e_l$  and beam helicity  $h_l/2$ :

$$d\sigma^{h_l, e_l}(\phi) = d\sigma_{UU}(\phi) [1 + h_l A_{LU, DVCS}(\phi) + e_l h_l A_{LU, I}(\phi) + e_l A_C(\phi)] ,$$

In HERMES - both longitudinally polarized positively and negatively charged beams were available:

$$A_C(\phi) = \frac{1}{4d\sigma_{UU}(\phi)} \left[ (d\sigma^{\rightarrow\rightarrow} + d\sigma^{\leftarrow\leftarrow}) - (d\sigma^{\rightarrow\leftarrow} + d\sigma^{\leftarrow\rightarrow}) \right] .$$

$$A_{LU, I}(\phi) = \frac{1}{4d\sigma_{UU}(\phi)} \left[ (d\sigma^{\rightarrow\rightarrow} - d\sigma^{\leftarrow\leftarrow}) - (d\sigma^{\rightarrow\leftarrow} - d\sigma^{\leftarrow\rightarrow}) \right] ,$$

$$A_{LU, DVCS}(\phi) = \frac{1}{4d\sigma_{UU}(\phi)} \left[ (d\sigma^{\rightarrow\rightarrow} - d\sigma^{\leftarrow\leftarrow}) + (d\sigma^{\rightarrow\leftarrow} - d\sigma^{\leftarrow\rightarrow}) \right] .$$

In Jefferson Lab, one can only measure the beam spin asymmetry  $A_{LU}^{e_l}$

$$A_{LU}^{e_l}(\phi) = \frac{d\sigma^{\rightarrow\leftarrow} - d\sigma^{\leftarrow\rightarrow}}{d\sigma^{\rightarrow\leftarrow} + d\sigma^{\leftarrow\rightarrow}} ,$$



## Observables

Target longitudinal spin asymmetry which reads :

$$A_{\text{UL}}^{e_l}(\phi) = \frac{[d\sigma^{\leftarrow \Rightarrow} + d\sigma^{\rightarrow \Rightarrow}] - [d\sigma^{\leftarrow \leftarrow} + d\sigma^{\rightarrow \leftarrow}]}{[d\sigma^{\leftarrow \Rightarrow} + d\sigma^{\rightarrow \Rightarrow}] + [d\sigma^{\leftarrow \leftarrow} + d\sigma^{\rightarrow \leftarrow}]},$$

where the double arrows  $\leftarrow (\Rightarrow)$  refer to the target polarization state parallel (anti-parallel) to the beam momentum. The double longitudinal target spin asymmetry is defined in a similar fashion :

$$A_{\text{LL}}^{e_l}(\phi) = \frac{[d\sigma^{\rightarrow \Rightarrow} + d\sigma^{\leftarrow \leftarrow}] - [d\sigma^{\leftarrow \Rightarrow} + d\sigma^{\rightarrow \leftarrow}]}{[d\sigma^{\rightarrow \Rightarrow} + d\sigma^{\leftarrow \leftarrow}] + [d\sigma^{\leftarrow \Rightarrow} + d\sigma^{\rightarrow \leftarrow}]},$$

The HERMES collaboration also had access to a transversally polarized target with both electrons and positrons:

$$A_{\text{UT,I}}(\phi, \phi_S) = \frac{d\sigma^+(\phi, \phi_S) + d\sigma^+(\phi, \phi_S + \pi) - d\sigma^-(\phi, \phi_S) - d\sigma^-(\phi, \phi_S + \pi)}{d\sigma^+(\phi, \phi_S) - d\sigma^+(\phi, \phi_S + \pi) + d\sigma^-(\phi, \phi_S) - d\sigma^-(\phi, \phi_S + \pi)},$$

$$A_{\text{UT,DVCS}}(\phi, \phi_S) = \frac{d\sigma^+(\phi, \phi_S) - d\sigma^+(\phi, \phi_S + \pi) - d\sigma^-(\phi, \phi_S) + d\sigma^-(\phi, \phi_S + \pi)}{d\sigma^+(\phi, \phi_S) - d\sigma^+(\phi, \phi_S + \pi) + d\sigma^-(\phi, \phi_S) - d\sigma^-(\phi, \phi_S + \pi)}$$

## Observables

$$\begin{aligned}
 A_C^{\cos \phi} &\propto \operatorname{Re} \left[ F_1 \mathcal{H} + \xi(F_1 + F_2) \tilde{\mathcal{H}} - \frac{t}{4m^2} F_2 \mathcal{E} \right], \\
 A_{LU,I}^{\sin \phi} &\propto \operatorname{Im} \left[ F_1 \mathcal{H} + \xi(F_1 + F_2) \tilde{\mathcal{H}} - \frac{t}{4m^2} F_2 \mathcal{E} \right], \\
 A_{UL,I}^{\sin \phi} &\propto \operatorname{Im} \left[ \xi(F_1 + F_2) \left( \mathcal{H} + \frac{\xi}{1+\xi} \mathcal{E} \right) + F_1 \tilde{\mathcal{H}} - \xi \left( \frac{\xi}{1+\xi} F_1 + \frac{t}{4M^2} F_2 \right) \tilde{\mathcal{E}} \right], \\
 A_{LL,I}^{\cos \phi} &\propto \operatorname{Re} \left[ \xi(F_1 + F_2) \left( \mathcal{H} + \frac{\xi}{1+\xi} \mathcal{E} \right) + F_1 \tilde{\mathcal{H}} - \xi \left( \frac{\xi}{1+\xi} F_1 + \frac{t}{4M^2} F_2 \right) \tilde{\mathcal{E}} \right], \\
 A_{LL,DVCS}^{\cos(0\phi)} &\propto \operatorname{Re} \left[ 4(1-\xi^2) (\mathcal{H} \tilde{\mathcal{H}}^* + \tilde{\mathcal{H}} \mathcal{H}^*) - 4\xi^2 (\mathcal{H} \tilde{\mathcal{E}}^* + \tilde{\mathcal{E}} \mathcal{H}^* + \tilde{\mathcal{H}} \mathcal{E}^* + \mathcal{E} \tilde{\mathcal{H}}^*) \right. \\
 &\quad \left. - 4\xi \left( \frac{\xi^2}{1+\xi} + \frac{t}{4M^2} \right) (\mathcal{E} \tilde{\mathcal{E}}^* + \tilde{\mathcal{E}} \mathcal{E}^*) \right], \\
 A_{UT,DVCS}^{\sin(\phi-\phi_s)} &\propto \left[ \operatorname{Im} (\mathcal{H} \mathcal{E}^*) - \xi \operatorname{Im} (\tilde{\mathcal{H}} \tilde{\mathcal{E}}^*) \right], \\
 A_{UT,I}^{\sin(\phi-\phi_s) \cos \phi} &\propto \operatorname{Im} \left[ -\frac{t}{4M^2} (F_2 \mathcal{H} - F_1 \mathcal{E}) + \xi^2 \left( F_1 + \frac{t}{4M^2} F_2 \right) (\mathcal{H} + \mathcal{E}) \right. \\
 &\quad \left. - \xi^2 (F_1 + F_2) \left( \tilde{\mathcal{H}} + \frac{t}{4M^2} \tilde{\mathcal{E}} \right) \right].
 \end{aligned} \tag{1}$$





| Experiment | Observable                                     | Normalized CFF dependence   |
|------------|--|---|
| HERMES     | $A_C^{\cos 0\phi}$                             | $\text{Re}\mathcal{H} + 0.06\text{Re}\mathcal{E} + 0.24\text{Re}\tilde{\mathcal{H}}$                                    |
|            | $A_C^{\cos \phi}$                              | $\text{Re}\mathcal{H} + 0.05\text{Re}\mathcal{E} + 0.15\text{Re}\tilde{\mathcal{H}}$                                    |
|            | $A_{\text{LU},\text{I}}^{\sin \phi}$           | $\text{Im}\mathcal{H} + 0.05\text{Im}\mathcal{E} + 0.12\text{Im}\tilde{\mathcal{H}}$                                    |
|            | $A_{\text{UL}}^{+,\sin \phi}$                  | $\text{Im}\tilde{\mathcal{H}} + 0.10\text{Im}\mathcal{H} + 0.01\text{Im}\mathcal{E}$                                    |
|            | $A_{\text{UL}}^{+,\sin 2\phi}$                 | $\text{Im}\tilde{\mathcal{H}} - 0.97\text{Im}\mathcal{H} + 0.49\text{Im}\mathcal{E} - 0.03\text{Im}\tilde{\mathcal{E}}$ |
|            | $A_{\text{LL}}^{+,\cos 0\phi}$                 | $1 + 0.05\text{Re}\tilde{\mathcal{H}} + 0.01\text{Re}\mathcal{H}$   |
|            | $A_{\text{LL}}^{+,\cos \phi}$                  | $1 + 0.79\text{Re}\tilde{\mathcal{H}} + 0.11\text{Im}\mathcal{H}$   |
|            | $A_{\text{UT,DVCS}}^{\sin(\phi-\phi_S)}$       | $\text{Im}\mathcal{H}\text{Re}\mathcal{E} - \text{Im}\mathcal{E}\text{Re}\mathcal{H}$                                   |
|            | $A_{\text{UT,I}}^{\sin(\phi-\phi_S)\cos \phi}$ | $\text{Im}\mathcal{H} - 0.56\text{Im}\mathcal{E} - 0.12\text{Im}\tilde{\mathcal{H}}$                                    |
| CLAS       | $A_{\text{LU}}^{-,\sin \phi}$                  | $\text{Im}\mathcal{H} + 0.06\text{Im}\mathcal{E} + 0.21\text{Im}\tilde{\mathcal{H}}$                                    |
|            | $A_{\text{UL}}^{-,\sin \phi}$                  | $\text{Im}\tilde{\mathcal{H}} + 0.12\text{Im}\mathcal{H} + 0.04\text{Im}\mathcal{E}$                                    |
|            | $A_{\text{UL}}^{-,\sin 2\phi}$                 | $\text{Im}\tilde{\mathcal{H}} - 0.79\text{Im}\mathcal{H} + 0.30\text{Im}\mathcal{E} - 0.05\text{Im}\tilde{\mathcal{E}}$ |
| HALL A     | $\Delta\sigma^{\sin \phi}$                     | $\text{Im}\mathcal{H} + 0.07\text{Im}\mathcal{E} + 0.47\text{Im}\tilde{\mathcal{H}}$                                    |
|            | $\sigma^{\cos 0\phi}$                          | $1 + 0.05\text{Re}\mathcal{H} + 0.007\mathcal{H}\mathcal{H}^*$  |
|            | $\sigma^{\cos \phi}$                           | $1 + 0.12\text{Re}\mathcal{H} + 0.05\text{Re}\tilde{\mathcal{H}}$   |
| HERA       | $\sigma_{\text{DVCS}}$                         | $\mathcal{H}\mathcal{H}^* + 0.09\mathcal{E}\mathcal{E}^* + \tilde{\mathcal{H}}\tilde{\mathcal{H}}^*$                    |

$$E_e = 5.75 \text{ GeV}, x_B = 0.36$$

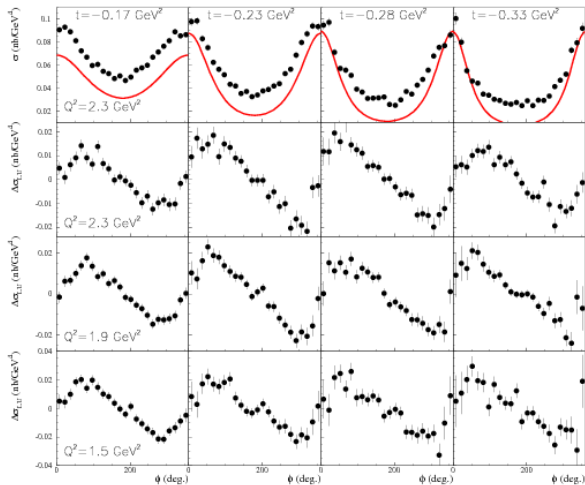


Figure: HALL A data. Red curve - pure BH contribution.



Topic for another seminar...

- ▶ A lot of data, but not enough to fit 4 GPDs (function of 3 variables) for every quark flavour ... and gluons
- ▶ GPDs must satisfy certain principles
- ▶ Few models on the market (Goloskokov-Kroll, VGG, Kumericki-Mueller ...), most of them describe data well (small problems with Hall A), only one describes all data - including small  $x$ .
- ▶ still much more data needed to determine GPDs (only imaginary part of CFF  $H$  determined with 15% precision, rest unconstrained)



## DATA vs models

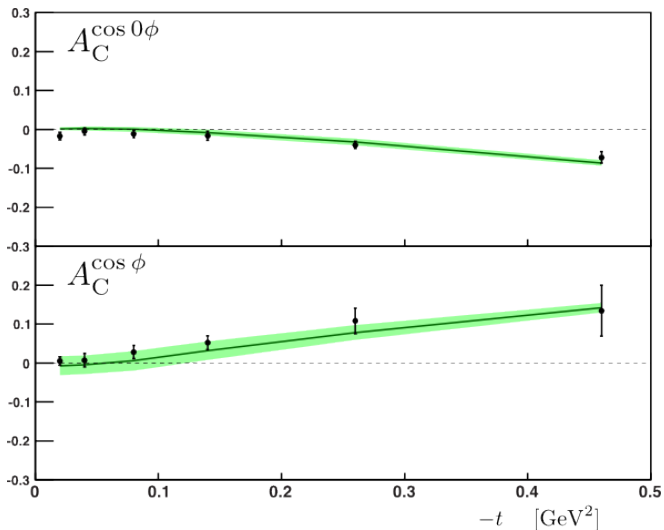
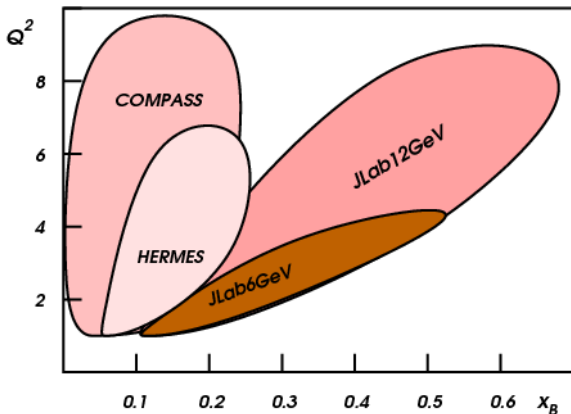


Figure: Harmonics of the beam charge asymmetry in HERMES:  $x_B = 0.097$  and  $Q^2 = 2.51 \text{ GeV}^2$  -compared to the Goloskokov - Kroll model.

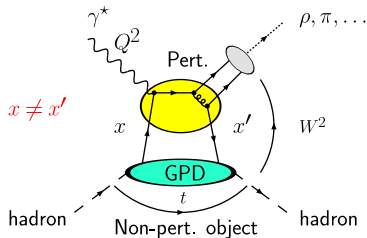
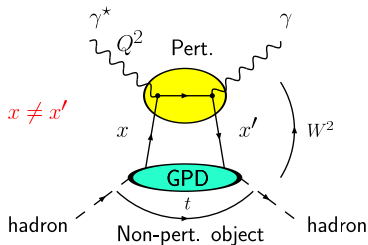
## FUTURE

- ▶ JLAB is in the upgrade phase - 12 GeV beam expected in 2015. Plans for Hall A and CLAS to measure beam spin and target spin asymmetries with much higher luminosity, smaller  $x_B$  and higher  $Q^2$ . Also CLAS plan to measure DVCS on neutron - necessary to make GPD flavour separation.
- ▶ COMPASS - recoil detector to ensure exclusivity - plans to measure mixed charge-spin asymmetries with 160 GeV muon beam.
- ▶ EIC (?)



## DVCS - what else, and why

- ▶ Difficult: exclusivity, 3 variables, GPD enter through convolutions, only  $GPD(\xi, \xi, t)$  accessible through DVCS at LO!
- ▶ universality,
- ▶ flavour separation,



- ▶ Meson production - additional information (and difficulties),



So, in addition to spacelike DVCS ...

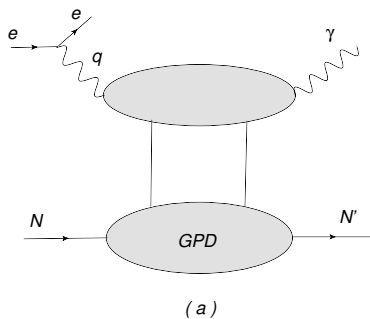


Figure: Deeply Virtual Compton Scattering (DVCS) :  $lN \rightarrow l'N'\gamma$



we can also study **timelike DVCS**

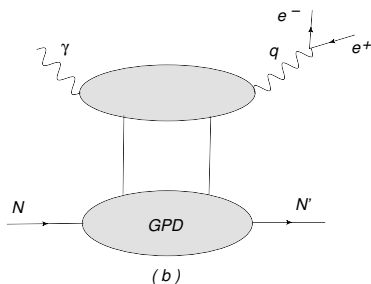


Figure: Timelike Compton Scattering (**TCS**):  $\gamma N \rightarrow l^+ l^- N'$

Why **TCS**:

- ▶ universality of the GPDs
- ▶ another source for GPDs (special sensitivity on real part of GPD  $H$ ),
- ▶ spacelike-timelike crossing,
- ▶ first step towards DDCVS,





## General Compton Scattering:

$$\gamma^*(q_{in})N(p) \rightarrow \gamma^*(q_{out})N'(p')$$

variables, describing the processes of interest in this generalized Bjorken limit, are the **scaling variable**  $\xi$  and **skewness**  $\eta > 0$ :

$$\xi = -\frac{q_{out}^2 + q_{in}^2}{q_{out}^2 - q_{in}^2}\eta, \quad \eta = \frac{q_{out}^2 - q_{in}^2}{(p + p') \cdot (q_{in} + q_{out})}.$$

- ▶ DDVCS:  $q_{in}^2 < 0$ ,  $q_{out}^2 > 0$ ,  $\eta \neq \xi$
- ▶ DVCS:  $q_{in}^2 < 0$ ,  $q_{out}^2 = 0$ ,  $\eta = \xi > 0$
- ▶ TCS:  $q_{in}^2 = 0$ ,  $q_{out}^2 > 0$ ,  $\eta = -\xi > 0$



## Coefficient functions and Compton Form Factors

CFFs are the GPD dependent quantities which enter the amplitudes. They are defined through relations:

$$\mathcal{A}^{\mu\nu}(\xi, \eta, t) = -e^2 \frac{1}{(P+P')^+} \bar{u}(P') \left[ g_T^{\mu\nu} \left( \mathcal{H}(\xi, \eta, t) \gamma^+ + \mathcal{E}(\xi, \eta, t) \frac{i\sigma^{+\rho} \Delta_\rho}{2M} \right) + i\epsilon_T^{\mu\nu} \left( \tilde{\mathcal{H}}(\xi, \eta, t) \gamma^+ \gamma_5 + \tilde{\mathcal{E}}(\xi, \eta, t) \frac{\Delta^+ \gamma_5}{2M} \right) \right] u(P),$$

,where:

$$\begin{aligned} \mathcal{H}(\xi, \eta, t) &= + \int_{-1}^1 dx \left( \sum_q T^q(x, \xi, \eta) H^q(x, \eta, t) + T^g(x, \xi, \eta) H^g(x, \eta, t) \right) \\ \tilde{\mathcal{H}}(\xi, \eta, t) &= - \int_{-1}^1 dx \left( \sum_q \tilde{T}^q(x, \xi, \eta) \tilde{H}^q(x, \eta, t) + \tilde{T}^g(x, \xi, \eta) \tilde{H}^g(x, \eta, t) \right). \end{aligned}$$

## ▶ DVCS vs TCS

$$\begin{aligned}
 DVCS T^q &= -e_q^2 \frac{1}{x+\eta-i\varepsilon} - (x \rightarrow -x) = (TCS T^q)^* \\
 DVCS \tilde{T}^q &= -e_q^2 \frac{1}{x+\eta-i\varepsilon} + (x \rightarrow -x) = -(TCS \tilde{T}^q)^*
 \end{aligned}$$

$$DVCS Re(\mathcal{H}) \sim P \int \frac{1}{x \pm \eta} H^q(x, \eta, t), \quad DVCS Im(\mathcal{H}) \sim i\pi H^q(\pm\eta, \eta, t)$$

## ▶ DDVCS

$$DDVCS T^q = -e_q^2 \frac{1}{x+\xi-i\varepsilon} - (x \rightarrow -x)$$

$$DDVCS Re(\mathcal{H}) \sim P \int \frac{1}{x \pm \xi} H^q(x, \eta, t), \quad DDVCS Im(\mathcal{H}) \sim i\pi H^q(\pm\xi, \eta, t)$$

But this is only true at LO. At NLO all GPDs hidden in the convolutions.



# TCS and Bethe-Heitler contribution to exclusive lepton pair photoproduction.

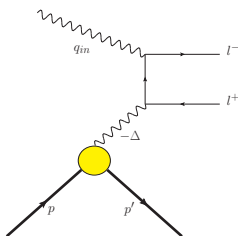


Figure: The Feynman diagram for the **Bethe-Heitler** amplitude.

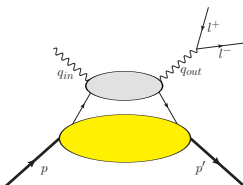


Figure: The Feynman diagram for the **Compton** amplitude.



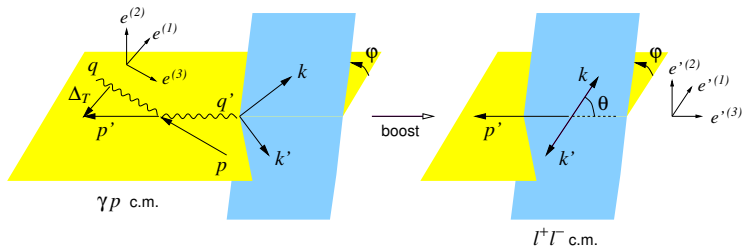
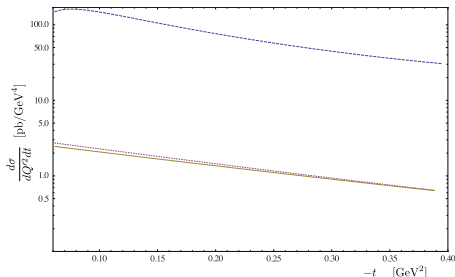


Figure: Kinematical variables and coordinate axes in the  $\gamma p$  and  $\ell^+ \ell^-$  c.m. frames.

# Interference

B-H dominant for not very high energies:



**Figure:** LO (dotted) and NLO (solid) TCS and Bethe-Heitler (dash-dotted) contributions to the cross section as a function of  $t$  for  $Q^2 = \mu^2 = 4 \text{ GeV}^2$  integrated over  $\theta \in (\pi/4; 3\pi/4)$  and over  $\phi \in (0; 2\pi)$  for  $E_\gamma = 10 \text{ GeV} (\eta \approx 0.11)$ .

The **interference** part of the cross-section for  $\gamma p \rightarrow l^+ l^- p$  with unpolarized protons and photons is given by:

$$\frac{d\sigma_{INT}}{dQ^2 dt d\cos\theta d\varphi} \sim \cos\varphi \cdot \text{Re}\mathcal{H}(\eta, t)$$

Linear in GPD's, odd under exchange of the  $l^+$  and  $l^-$  momenta  $\Rightarrow$  angular distribution of lepton pairs is a good tool to study interference term.



Rafael Paremuzyan PhD thesis

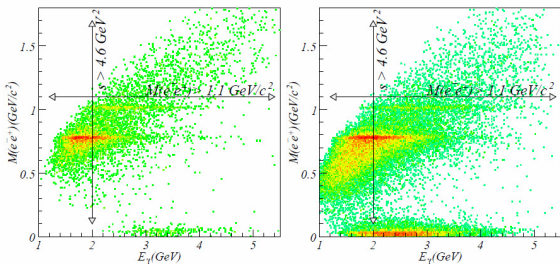


**Figure:**  $e^+e^-$  invariant mass distribution vs quasi-real photon energy. For TCS analysis  $M(e^+e^-) > 1.1 \text{ GeV}$  and  $s_{\gamma p} > 4.6 \text{ GeV}^2$  regions are chosen. Left graph represents e1-6 data set, right one is from e1f data set.



## Theory vs experiment

R.Paremuzyan and V.Guzey:

$$R = \frac{\int d\phi \cos \phi \int d\theta d\sigma}{\int d\phi \int d\theta d\sigma}$$

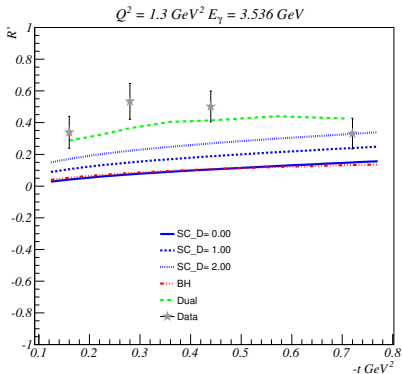


Figure: Theoretical prediction of the ratio  $R$  for various GPDs models. Data points after combining both e1-6 and e1f data sets.





**Jefferson Lab PAC 39 Proposal**  
**Timelike Compton Scattering and  $J/\psi$  photoproduction on the proton**  
**in  $e^+e^-$  pair production with CLAS12 at 11 GeV**

I. Albayrak,<sup>1</sup> V. Burkert,<sup>2</sup> E. Chudakov,<sup>2</sup> N. Dashyan,<sup>3</sup> C. Desnault,<sup>4</sup> N. Gevorgyan,<sup>3</sup>  
Y. Ghandilyan,<sup>3</sup> B. Guegan,<sup>4</sup> M. Guidal\*,<sup>4</sup> V. Guzey,<sup>2,5</sup> K. Hicks,<sup>6</sup> T. Horn\*,<sup>1</sup> C. Hyde,<sup>7</sup>  
Y. Ilieva,<sup>8</sup> H. Jo,<sup>4</sup> P. Khetarpal,<sup>9</sup> F.J. Klein,<sup>1</sup> V. Kubarovsky,<sup>2</sup> A. Marti,<sup>4</sup> C. Munoz Camacho,<sup>4</sup>  
P. Nadel-Turonski\*,<sup>2</sup> S. Niccolai,<sup>4</sup> R. Parendyan\*,<sup>4,3</sup> B. Pire,<sup>10</sup> F. Sabatié,<sup>11</sup> C. Salgado,<sup>12</sup>  
P. Schweitzer,<sup>13</sup> A. Simonyan,<sup>3</sup> D. Sokhan,<sup>4</sup> S. Stepanyan\*,<sup>2</sup> L. Szymanowski,<sup>14</sup>  
H. Voskanyan,<sup>3</sup> J. Wagner,<sup>14</sup> C. Weiss,<sup>2</sup> N. Zachariou,<sup>8</sup> and the CLAS Collaboration.

<sup>1</sup>*Catholic University of America, Washington, D.C. 20064*

<sup>2</sup>*Thomas Jefferson National Accelerator Facility, Newport News, Virginia 23606*

<sup>3</sup>*Yerevan Physics Institute, 375036 Yerevan, Armenia*

<sup>4</sup>*Institut de Physique Nucleaire d'Orsay, IN2P3, BP 1, 91406 Orsay, France*

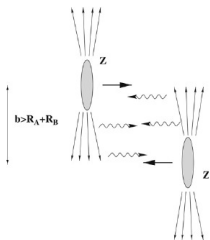
<sup>5</sup>*Hampton University, Hampton, Virginia 23668*

<sup>6</sup>*Ohio University, Athens, Ohio 45701*

Approved experiment at Hall B, and LOI for Hall A.



## Ultraperipheral collisions



$$\sigma_{pp} = 2 \int \frac{dn(k)}{dk} \sigma_{\gamma p}(k) dk$$

$\sigma_{\gamma p}(k)$  is the cross section for the  $\gamma p \rightarrow pl^+l^-$  process and  $k$  is the  $\gamma$ 's energy.

$\frac{dn(k)}{dk}$  is an equivalent photon flux

$$\frac{dn(k)}{dk} = \frac{\alpha}{2\pi k} \left[ 1 + \left( 1 - \frac{2k}{\sqrt{s_{pp}}} \right)^2 \right] \left( \ln A - \frac{11}{6} + \frac{3}{A} - \frac{3}{2A^2} + \frac{1}{3A^3} \right)$$

$A = 1 + \frac{0.71 \text{ GeV}^2}{Q_{min}^2}$ ,  $Q_{min}^2 \approx \frac{4M_p^2 k^2}{s_{pp}}$  is the minimal  $-t$

$s_{pp}$  is the proton-proton energy squared ( $\sqrt{s_{pp}} = 14 \text{ TeV}$ ):  $s \approx 2\sqrt{s_{pp}}k$



## B-H cross section at UPC

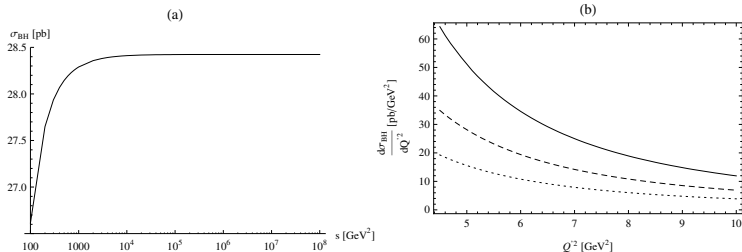


**Figure:** (a) The BH cross section integrated over  $\theta \in [\pi/4, 3\pi/4]$ ,  $\varphi \in [0, 2\pi]$ ,  $Q'^2 \in [4.5, 5.5] \text{ GeV}^2$ ,  $|t| \in [0.05, 0.25] \text{ GeV}^2$ , as a function of  $\gamma p$  c.m. energy squared  $s$ . (b) The BH cross section integrated over  $\varphi \in [0, 2\pi]$ ,  $|t| \in [0.05, 0.25] \text{ GeV}^2$ , and various ranges of  $\theta$ :  $[\pi/3, 2\pi/3]$  (dotted),  $[\pi/4, 3\pi/4]$  (dashed) and  $[\pi/6, 5\pi/6]$  (solid), as a function of  $Q'^2$  for  $s = 10^5 \text{ GeV}^2$



## TCS cross section at UPC

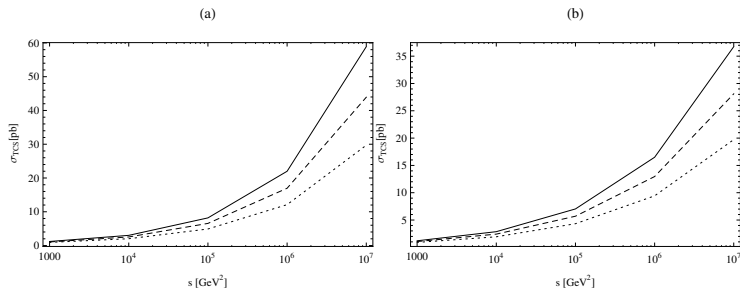


**Figure:**  $\sigma_{TCS}$  as a function of  $\gamma p$  c.m. energy squared  $s$ , for GRVGJR2008 LO (a) and NLO (b) parametrizations, for different factorization scales  $\mu_F^2 = 4$  (dotted), 5 (dashed), 6 (solid)  $\text{GeV}^2$ .

For very high energies  $\sigma_{TCS}$  calculated with  $\mu_F^2 = 6 \text{ GeV}^2$  is much bigger than with  $\mu_F^2 = 4 \text{ GeV}^2$ . Also predictions obtained using LO and NLO GRVGJR2008 PDFs differ significantly.



# The interference cross section at UPC

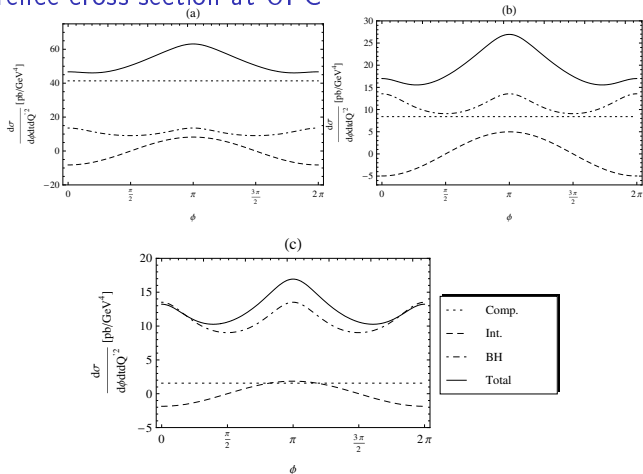


**Figure:** The differential cross sections (solid lines) for  $t = -0.2 \text{ GeV}^2$ ,  $Q'^2 = 5 \text{ GeV}^2$  and integrated over  $\theta = [\pi/4, 3\pi/4]$ , as a function of  $\phi$ , for  $s = 10^7 \text{ GeV}^2$  (a),  $s = 10^5 \text{ GeV}^2$  (b),  $s = 10^3 \text{ GeV}^2$  (c) with  $\mu_F^2 = 5 \text{ GeV}^2$ . We also display the Compton (dotted), Bethe-Heitler (dash-dotted) and Interference (dashed) contributions.

The pure Bethe - Heitler contribution to  $\sigma_{pp}$ , integrated over  $\theta = [\pi/4, 3\pi/4]$ ,  $\phi = [0, 2\pi]$ ,  $t = [-0.05 \text{ GeV}^2, -0.25 \text{ GeV}^2]$ ,  $Q'^2 = [4.5 \text{ GeV}^2, 5.5 \text{ GeV}^2]$ , and photon energies  $k = [20, 900] \text{ GeV}$  gives:

$$\sigma_{pp}^{BH} = 2.9 \text{ pb} .$$

The Compton contribution (calculated with NLO GRVGJR2008 PDFs, and  $\mu_F^2 = 5 \text{ GeV}^2$ ) gives:

$$\sigma_{pp}^{TCS} = 1.9 \text{ pb} .$$

LHC: rate  $\sim 10^5$  events/year with nominal luminosity ( $10^{34} \text{ cm}^{-2}\text{s}^{-1}$ )



# Ultrapерipheral collisions at RHIC

$$L \cdot k \frac{dn}{dk} (\text{mb}^{-1} \text{sec}^{-1})$$

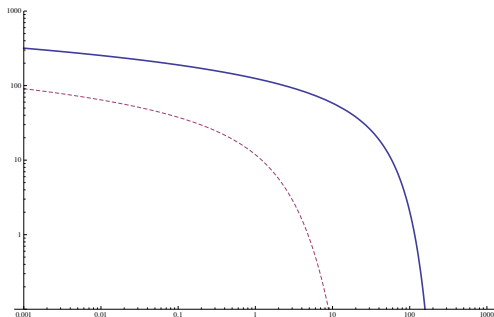


**Figure:** Effective luminosity of the photon flux from the Au-Au (dashed) and proton-proton (solid) collisions as a function of photon energy  $k$ (GeV).



$$\frac{d\sigma^{AuAu}}{dQ^2 dt d\phi} (\mu\text{b GeV}^{-4})$$

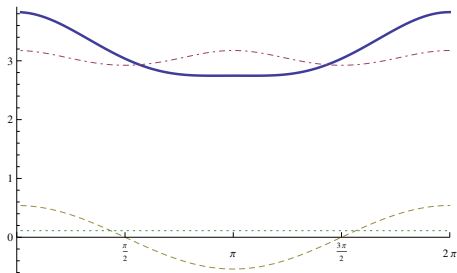


**Figure:** The differential cross sections (solid lines) for  $t = -0.1 \text{ GeV}^2$ ,  $Q'^2 = 5 \text{ GeV}^2$  and integrated over  $\theta = [\pi/4, 3\pi/4]$ , as a function of  $\varphi$ . We also display the Compton (dotted), Bethe-Heitler (dash-dotted) and Interference (dashed) contributions.

Total BH cross section (for  $Q \in (2, 2.9) \text{ GeV}$ ,  $t \in (-0.2, -0.05) \text{ GeV}^2$ ,  $\theta = [\pi/4, 3\pi/4]$  and  $\phi \in (0, 2\pi)$ )

$$\sigma_{BH} = 41 \mu\text{b}$$





$$\frac{d\sigma^{PP}}{dQ^2 dt d\phi} \text{ (pb GeV}^{-4}\text{)}$$

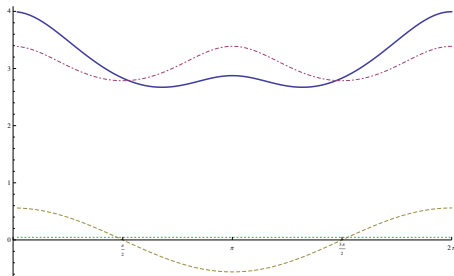


**Figure:** The differential cross sections (solid lines) for  $t = -0.1 \text{ GeV}^2$ ,  $Q'^2 = 5 \text{ GeV}^2$  and integrated over  $\theta = [\pi/4, 3\pi/4]$ , as a function of  $\varphi$ . We also display the Compton (dotted), Bethe-Heitler (dash-dotted) and Interference (dashed) contributions.

Total BH cross section (for  $Q \in (2, 2.9) \text{ GeV}$ ,  $t \in (-0.2, -0.05) \text{ GeV}^2$ ,  $\theta = [\pi/4, 3\pi/4]$  and  $\phi \in (0, 2\pi)$ )

$$\sigma_{BH} = 9\text{pb}$$



## AFTER - a fixed target experiment using LHC beams.

→ see Jean-Philippe Lansberg talk on Wednesday

For fixed  $t$  and  $Q^2$ ,  $k_\gamma(y)$  is also fixed:

$$\begin{aligned}d\sigma^{hh} &= \int dk_\gamma \frac{dn}{dk_\gamma} d\sigma^{\gamma h}(s^{\gamma h}(k_\gamma)) \\ &= \int dy \frac{dn}{dy} d\sigma^{\gamma h}(s^{\gamma h}(k_\gamma(y))),\end{aligned}$$

and

$$\frac{d\sigma^{hh}}{dy} = \frac{dn}{dy} d\sigma^{\gamma h}(s^{\gamma h}(k_\gamma(y))).$$



# AFTER

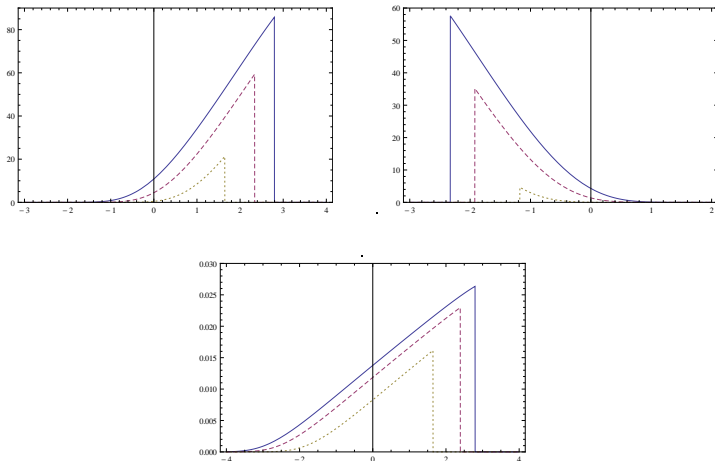
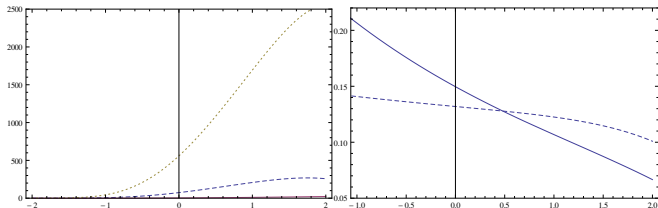
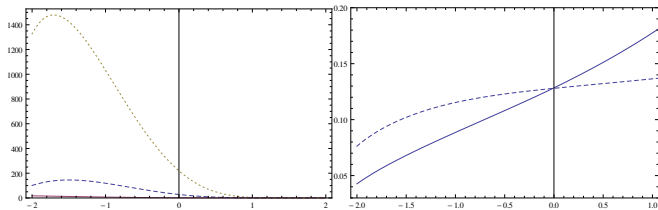


Figure:  $\frac{dn}{dy}$  for the proton run on Pb nucleon target (left), and for Pb run on H target (right), and for p-p run (target proton treated as a source of WW photons). The flux is calculated for  $Q^2 = 4 \text{ GeV}^2$ ,  $t = -0.1 \text{ GeV}^2$  up to the kinematical threshold implicitly set by  $Q^2$ .





(a) 7 TeV  $p$  run on Pb target



(b) 2.76 TeV Pb on H target

**Figure:** (left)  $\frac{d\sigma}{dy}$  and ratio for the KG model for  $Q^2 = 4 \text{ GeV}^2$ ,  $t = -0.1 \text{ GeV}^2$  and  $\phi = 0$  integrated over  $\theta \in (\pi/4, 3\pi/4)$ . Dotted line :BH, dashed line :interference term, solid line: TCS. (right) Ratio of the interference BH-DVCS to BH calculated for  $Q^2 = 4 \text{ GeV}^2$ ,  $t = -0.1 \text{ GeV}^2$  and  $\phi = 0$  for the GK model (dashed) and a model based on MSTW08 (solid).

# Gluon GPDs in the UPC production of heavy mesons

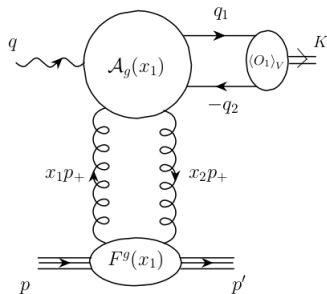


Figure 1: Kinematics of heavy vector meson photoproduction.

- ▶ Theoretical framework for GPD description of heavy meson photoproduction set with NLO accuracy by: D. Yu. Ivanov , A. Schafer , L. Szymanowski and G. Krasnikov - **Eur.Phys.J. C34 (2004) 297-316**
- ▶ Skewness effects directly taken into account.
- ▶ Big sensitivity to the factorization scale - situation better for  $\Upsilon$  than for  $J/\psi$ .
- ▶ UPC - work in progress with D.Yu.Ivanov and L.Szymanowski



## Summary

- ▶ GDPs enter factorization theorems for hard exclusive reactions (DVCS, deeply virtual meson production etc.), in a similar manner as PDFs enter factorization theorem for DIS
- ▶ First moment of GPDs enter the Ji's sum rule for the angular momentum carried by partons in the nucleon.
- ▶ Fourier transform of GPD's to impact parameter space can be interpreted as „tomographic” 3D pictures of nucleon, describing charge distribution in the transverse plane, for a given value of  $x$ .
- ▶ A lot of data on DVCS, but not enough to determine GPDs,
- ▶ A lot of new experiments planned to measure DVCS - JLAB 12, COMPASS, EIC(?),
- ▶ Timelike-DVCS is a complementary measurement,
- ▶ TCS already measured at JLAB 6 GeV, but much richer and more interesting kinematical region available after upgrade to 12 GeV, maybe possible at COMPASS.
- ▶ Compton scattering in ultraperipheral collisions at hadron colliders opens a new way to measure generalized parton distributions
- ▶ NLO corrections very important, also important for GPD extraction at  $\xi \neq x$ .

